

Non-metal Doped TiO₂ films as Visible-light Photocatalysts by Physical Vapor Deposition

Tien-Syh Yang(楊天賜)^{a*}, Shi-Jie Shen(沈士傑)^b, Ming-Show Wong(翁明壽)^b

^a General Educational Center, Tzu Chi College of Technology, Hualien 97005 Taiwan

^b Department of Materials Science and Engineering, National Dong Hwa University, Hualien 97401, Taiwan

*Email: tsyang@ems.tccn.edu.tw

Abstract

Non-metal (B-, C-, N-) doping into TiO₂ to promote the photocatalytic activities under visible light has been actively pursued in recent years. Physical vapor deposition methods were used to prepare TiO₂-based films with distinct chemical structures and electronic natures of the dopant species, which would induce red-shifted absorption and improve photocatalytic activities. B-TiO₂ films were prepared by reactive magnetron co-sputtering two targets of Ti and TiB₂ in Ar and O₂ atmosphere. C-TiO₂ films were deposited by two processes: one by ion-assisted electron-beam evaporation of TiO₂ powder source material and CO or CO₂ as the feed gas for the ion gun, the other by reactive magnetron co-sputtering of Ti and graphite targets in Ar and O₂ gases. N-TiO₂ films were also deposited by ion-assisted electron-beam evaporation using TiO₂ powder source material and N₂ as the feed gas for the ion gun, and by reactive magnetron sputtering of a Ti target in Ar, O₂ and N₂ mixtures, respectively. Various dopant species in the films were detected and characterized, and the main species, which were responsible for the red-shift absorption to visible-light and the promotion of the photocatalytic activities, were identified.

Keywords: Titanium oxide; Non-metal doping; Physical vapor deposition; Photocatalytic activity (Photocatalysis)

NSC Project no.: NSC102-2221-E-259-005-MY3

1 Introduction

Titanium oxide (TiO₂) is known as the most useful photocatalyst because of its special optical and electronic properties, low cost, chemical stability and nontoxicity [1–4]. Despite the broad photocatalytic applications for TiO₂, two major defects exist: the larger energy band gap and the higher recombination rate, which obstructs the exploitation of solar light and causes the low quantum efficiency in photocatalytic reactions [5,6]. Therefore, considerable efforts have been made to extend the photoresponse further into the visible-light region. Non-metals doping, especially for nitrogen (N) and carbon (C), have been considered for about ten years as a prevailing way to change the photo-absorption properties of TiO₂ for harvesting solar light with applications in photocatalysis [7–10].

Problems associated with the removal of the suspended TiO₂ particles in liquid after the photocatalysis have led to increased attention on the colloidal films immobilized on substrates. The fixation of previously prepared TiO₂ powder used various techniques such as silane coupling, immobilization in a polymer matrix, electrophoretic deposition over conducting substrates, dip coating and spin coating to prepare the films [11–14]. However, TiO₂ thin films in optical and biocompatible applications were prepared preferentially by the dry processes as physical vapor depositions [15–17]. Among them, electron-beam evaporation and magnetron sputtering were powerful techniques to prepare well-crystallized oxide films with higher deposition rate and controlled stoichiometry by adjusting some instrumental parameters [18–19].

The introduction of non-metal dopant in the lattice may affect the band edges or introduce impurity states in the band gaps of the system [20]. The description of these effects is very delicate from the experimental and theoretical views, especially concerning the localized or delocalized nature of the impurity states [21]. In fact, the insertion of dopant impurities into the oxide structure may also increase the rate of the undesired recombination of photocatalytically generated charge carriers, which is known to become less favored, the higher is the crystallinity degree of the oxide structure. We have used successfully the reactive magnetron sputtering deposition and ion-assisted electron-beam evaporation to deposit N-TiO₂ [17,22-23], C-TiO₂ [16, 24-25] and B-TiO₂ in our laboratory, and investigated in detail the phase structures of TiO₂ and chemical states of the dopant species, and the correlation with the improvement of the photocatalytic activity under UV or Visible irradiation. Both substitutional to O or interstitial dopants in the anatase lattice have been considered. In this work we present a systematic comparative study of the non-metal doping of TiO₂ by some elements of the second row of the periodic table (B, C, N). The main aim of this study is to identify and rationalize the roles of the dopants.

2 Experimental

The ion-assisted electron-beam evaporation and reactive magnetron sputtering systems allows independent control of several critical deposition parameters and the details of the system were described in Figure 1 and Figure 2, respectively. B-TiO₂ films were prepared by reactive magnetron co-sputtering two targets of Ti and TiB₂ in Ar and O₂ atmosphere. C-TiO₂ films were deposited by two processes: one by ion-assisted electron-beam evaporation of TiO₂ powder source material and CO or CO₂ as the feed gas for the ion gun, the other by reactive magnetron co-sputtering of Ti and graphite targets in Ar and O₂ gases. N-TiO₂ films were also deposited by ion-assisted electron-beam evaporation using TiO₂ powder source material and N₂ as the feed gas for the ion gun, and by reactive magnetron sputtering of a Ti target in Ar, O₂ and N₂ mixtures, respectively.

The structure and crystallinity of the films were determined

by X-ray diffractometer (XRD). The surface composition and bonding of the films were detected by an X-ray photoelectron spectroscopy (XPS). The photocatalytic property under visible-light illumination was evaluated by measuring decomposition rate of methylene blue (MB), monitored by the absorption peak around 664 nm in UV-Vis spectra.

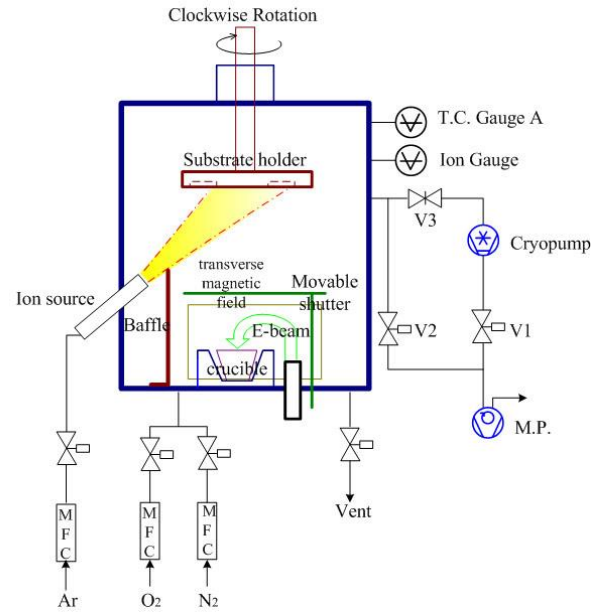


Figure 1: The ion-assisted electron-beam evaporation system.

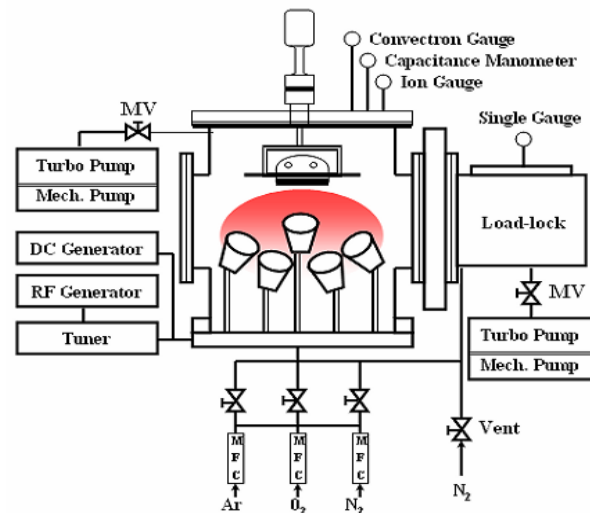


Figure 2: The reactive magnetron sputtering system.

3 Results and Discussions

3.1 N-TiO₂

3.1.1 By ion-assisted electron-beam evaporation [17, 23]

The N-TiO₂ films made the absorption edge of TiO₂ red-shifted to 500 nm and exhibited visible light-induced photocatalytic activities in the surface hydrophilicity and the degradation of MB. Figure 3 shows the N 1s XPS spectra of the N-TiO₂ films. The spectra exhibited two peaks around 403.1 and 396.3 eV as the N content above 2.5 at.% (Fig. 3b–d). The peak at 403.1 eV was assigned to chemisorbed molecular γ -N₂, and 396.3 eV to atomic β -N states (substitutional N). While the N loading up to 5.6 at.%, the β -N peak shifts to 396.9 eV as the formation of TiN. The substitutional N, which was readily doped by the energetic nitrogen ions from the ion gun, in anatase TiO₂ can increase visible light photocatalysis. The best photocatalytic activity was obtained at the largest N loading about 5.6 at.%, corresponding to the most substitutional N in anatase TiO₂. The film exhibited the degradation of MB with a rate-constant (k) about 0.293 h⁻¹ and retaining 3° water contact angle on the surface under visible light illumination.

3.1.2 By reactive magnetron sputtering [22]

Two types of nitrogen species are formed in the N-TiO₂ films following the fraction of N₂ (F_{N2}) in the reactive atmosphere. One is substitutional nitrogen in anatase titania phase and the other is nitrogen in TiN phase. In comparison with the previous study, the N-TiO₂ films deposited by ion-assisted electron-beam evaporation showed another N1s peak around 403.1 eV assigned as γ -N₂, which does not appear in the N-TiO₂ films by the magnetron sputtering deposition. The results suggested that the N₂⁺ ions with lower bombarding energies in the sputtering plasma were not apt to be implanted into the film to form γ -N₂ like those through the ion gun. In a range of F_{N2} from 0 to 0.57, about 1.0~1.4 at.% substitutional N were incorporated by energetic nitrogen ions in the sputtering plasma. The substitutional N red shifted to 500 nm from 380 nm of TiO₂ and exhibited photocatalytic properties under visible light. The best photocatalytic activity with a rate-constant (k) about 0.059~0.077 h⁻¹ was obtained at 1.0~1.4 at.%

substitutional N. The photocatalytic activities of the sputtered films were inferior to those of the ion-assisted evaporated films due to the lower substitutional N. When excess nitrogen was supplied as the F_{N2} above 0.75, the resulting film contained 20.8 at.% of nitrogen with the formation of TiN that makes the film opaque and destroys the photocatalytic activity largely.

3.2 C-TiO₂

3.2.1 By ion-assisted electron-beam evaporation [16, 25]

Figure 4 shows the C 1s XPS spectra of the C-TiO₂ films. The spectrum shows a broad band with the binding energies around 285 eV, assigned to C–C bonds. After Ar⁺ ion sputtering of the sample for 300 s, corresponding to an etching depth about 5 nm, the peak around 285 eV disappears and another peak around 282.6 eV emerges, assigned to Ti–C bond by substitution of lattice oxygen by carbon. The intensity of peak around 282.6 eV approaches a maximum and maintains a fixed value after etching for a depth of 20 nm (1200 s of sputtering).

C-TiO₂ films were prepared under the bombardment of CO ion beam with a fixed voltage of 1000 V and various beam currents of 10, 20 and 35 mA. As-deposited films had the primary structure of anatase TiO₂. With the increasing ion-beam current, the film crystallinity deteriorated, the concentration of carbon with Ti–C bonding in the films varied from 0.8 to 1.3 mol%, and their optical absorption edges gradually red-shifted from 370 to 410 nm. The C-TiO₂ film deposited with 10 mA beam current had well-crystallized anatase phase, exhibiting the highest water-contact angle reduction and the best visible-light photocatalytic activity with a rate constant about 0.084 h⁻¹.

More carbon content was incorporated when ion beam current was raised and when CO₂ gas was utilized as the ion source and it also resulted in shifting the absorbance edge of TiO₂ towards higher wavelength about 430 nm. The C-TiO₂ film of well-crystallized anatase phase with 1.25 at.% carbon dopant from CO₂ source exhibited the lowest contact-angle close to zero and the best photocatalytic activities in terms of the reduction of silver ions to metallic silver and the MB degradation under visible-light

illumination with a rate constant about 0.108 h^{-1} . Post annealing the films at a higher temperature (500°C) also improved the photocatalytic activities of the MB degradation with a rate constant about 0.170 h^{-1} .

3.2.2 By reactive magnetron sputtering [24, 26]

Figure 5 shows the C 1s XPS spectra of the C-TiO₂ films deposited with various graphite target power. The incorporation of carbon into TiO₂ retained the crystallinity of anatase phase and a mix of graphitic and substitutional carbon in nature, corresponding to 284.6 and 281.8 eV, respectively. The microstructure consisted of columnar carbon-doped titania grains covered with graphitic carbon along the grain boundaries. The films exhibited an absorption edge red shifted up to $\sim 450 \text{ nm}$ corresponding to a band gap $\sim 2.7 \text{ eV}$ and while absorption tails continued to above 700 nm . The films possessed outstanding visible light-induced photocatalytic properties in the reduction of silver ions, degradation of methylene blue and superhydrophilicity. The best photocatalytic activity was obtained in the C-TiO₂ film of the most carbon concentration about 9.3 at.% with a degradation rate-constant of 0.108 h^{-1} for MB under visible-light illumination.

3.3 B-TiO₂

3.3.1 By reactive magnetron sputtering

As-deposited B-TiO₂ films had no apparently photocatalytic activity with rate constants below 0.01 h^{-1} for MB degradation. However, the annealed B-TiO₂ films at 600°C for 1 hr possessed enhanced UV-induced photocatalytic activity about 10 times, and Visible-induced activity about 3 times. The annealed B-TiO₂ films had more and more pores as the TiB₂ target powers increased successively above 90 W, because more and more volatile B₂O₃ species depart from the films during annealing. The pores created more surface areas of anatase TiO₂ leading to higher UV-induced photocatalytic activity. Figure 6 shows the B 1s XPS spectra of the B-TiO₂ films after annealed. The spectra of the B-TiO₂ films with TiB₂ target powers around 30~90 W exhibited a peak at 191.4 eV, assigned as the interstitial B in literature (Fig. 6a–c). The peak at 191.4

eV may co-exist with other peaks at higher BE (192.5, 193.0~193.5eV) in the B-TiO₂ films by the powers above 90 W, indicating the possible formation of B₂O₃ microaggregates into or at the surface of the TiO₂ structure. Nevertheless, the interstitial B in anatase TiO₂ would enhance the Visible-induced photocatalytic activity.

4 Conclusion

From the results, non-metal (B-, C-, N-) doping into TiO₂ may promote the photocatalytic activities under visible light. Various doping species (substitutional N, substitutional C and interstitial B) related to the visible induced activities were found. Among them, the best photocatalytic activity was obtained in the N-TiO₂ film prepared by ion-assisted electron-beam evaporation. The N-TiO₂ film with the largest N loading about 5.6 at.%, corresponding to the most substitutional N in anatase TiO₂ and red-shift to 500 nm, exhibited the most degradation of MB with a rate-constant (k) about 0.293 h^{-1} and retaining 3° water contact angle on the surface under visible light illumination.

Acknowledgments

We appreciate the financial support of this study by National Science Foundation of Taiwan, ROC, under grant No. NSC 102-2221-E-259-005-MY3.

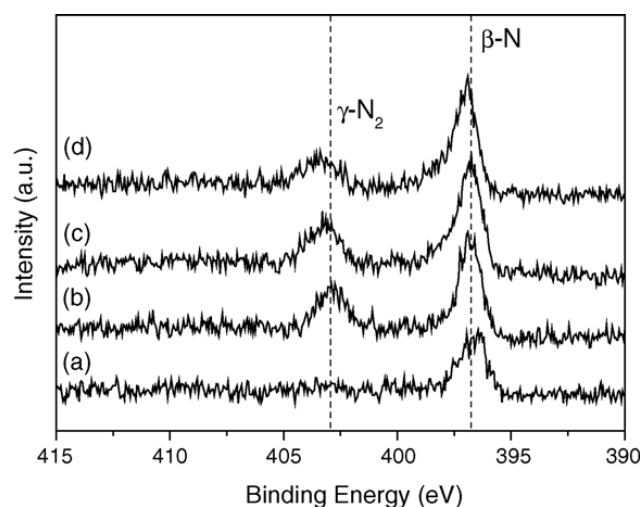


Figure 3: N 1s XPS spectra of the N-TiO₂ films: (a) TiON-2, (b) TiON-4, (c) TiON-15, and (d) TiON-25.

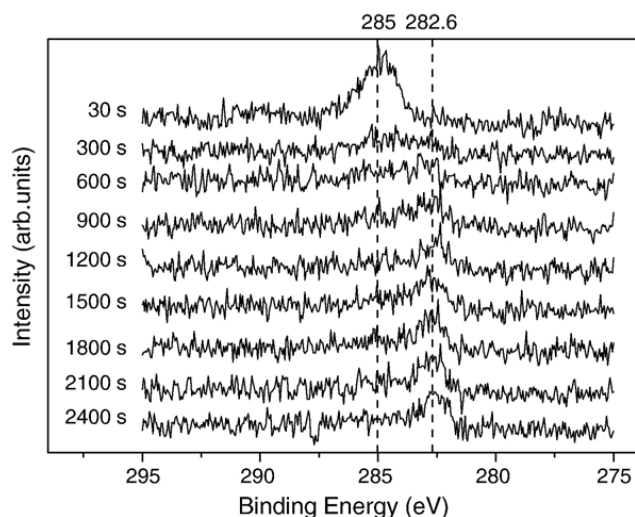


Figure 4: Depth profile of the C1s XPS spectra for the C-TiO₂ film by ion-assisted electron-beam evaporation.

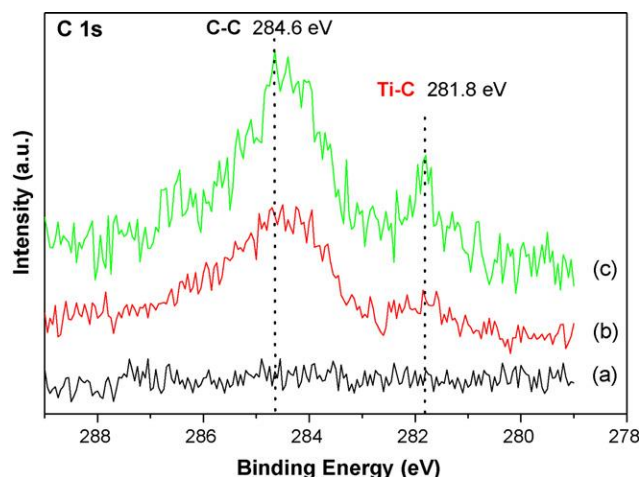


Figure 5: C 1s XPS spectra of the C-TiO₂ films with different graphite target powers in reactive magnetron sputtering system: (a) 0, (b) 200, (c) 350 W.

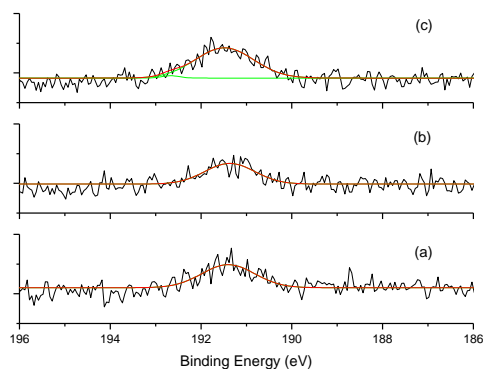


Figure 6: B 1s XPS spectra of the B-TiO₂ films with different TiB₂ target powers in reactive magnetron sputtering system: (a) 30, (b) 60, (c) 90, (d) 120, (e) 150, (f) 180 W.

References

- [1] A. Fujishima, T.N. Rao, D.A. Tryk, J. Photochem. Photobiol. C: Photochem. Rev. 1 (2001) 1.
- [2] M. R. Hoffmann, S. T. Martin, W. Choi, D. W. Bahnemann, Chem. Rev. 95 (1995) 69.
- [3] Khaselev, J.A. Turner, Science 280 (1998) 425.
- [4] W. M. Campbell, A. K. Burrell, D. L. Officer, K. W. Jolley, Coord. Chem. Rev. 248 (2004) 817.
- [5] C.C. Chen, W.H. Ma, J.C. Zhao, Chem. Soc. Rev. 39 (2010) 4206.
- [6] X. Chen, S. Shen, L. Guo, S.S. Mao, Chem. Rev. 110 (2010) 6503.
- [7] R. Asahi, T. Morikawa, T. Ohwaki, K. Aoki, Y. Taga, Science 293 (2001) 269.
- [8] X. Chen, S.S. Mao, Chem. Rev. 107 (2007) 2891.
- [9] A. Fujishima, X. Zhang, D.A. Tryk, Surf. Sci. Rep. 63 (2008) 515.
- [10] M.A. Henderson, Surf. Sci. Rep. 66 (2011) 185.
- [11] K. Tenakone, C.T.K. Tilakaratne, I.R.M. Kottegoda, J. Photochem. Photobiol. A: Chem. 87 (1995) 177.
- [12] I.M. Butterfield, P.A. Cristtensen, A. Hamnett, K.E. Shaw, G.M. Walker, S.A. Walker, J. Appl. Electrochem.

27 (1997) 385.

- [13] N. Negishi, K. Takeuchi, T. Ibusuki, Appl. Surf. Sci. 121 (1997) 417.
- [14] J.A. Byrne, B.R. Eggins, N.M.D. Brown, B. Mckinney, M. Rouse, Appl. Catal. 17 (1998) 25.
- [15] X. Wang, F. Zhang, Z. Zheng, C. Li, L. Chen, H. Wang, X. Lui, Mater. Lett. 44 (2000) 105.
- [16] S.W. Hsu, T.S. Yang, T.K. Chen, M.S. Wong, Thin Solid Films 515 (2007) 3521.
- [17] T.S. Yang, M.C. Yang, C.B. Shu, W.K. Chang and M.S. Wong, Appl. Surf. Sci. 252 (2006) 3729.
- [18] F. Lapostolle, A. Billard, J. von Stebut, Surf. Coat. Technol. 135 (2000) 1.
- [19] T.S. Yang, C.B. Shiu, M.S. Wong, Surf. Sci. 548 (2004) 75.
- [20] C. Di Valentin, G. Pacchioni, A. Selloni, Phys. Rev. B 70 (2004) 085116.
- [21] C. Di Valentin, G. Pacchioni, A. Selloni, J. Phys. Chem. C 113 (2009) 20543.
- [22] M.S. Wong, S.B. Chou, T.S. Yang, Thin Solid Films 494 (2006) 244.
- [23] M.C. Yang, T.S. Yang, M.S. Wong, Thin Solid Films 469-470 (2004) 1.
- [24] S.H. Wang, T.K. Chen, K.K. Rao, M.S. Wong, Appl. Catal. B: Environ. 76 (2007) 328.
- [25] M.S. Wong, S.W. Hsu, K.K. Rao, C.P. Kumar, J. of Mol. Catal. A: Chem. 279 (2008) 20.
- [26] M.S. Wong, S.H. Wang, T.K. Chen, C.W. Weng, K.K. Rao, Surf. and Coat. Techn. 202 (2007) 890.